J Mater Sci (2010) 45:4180–4187
DOI 10.1007/s10853-010-4508-2

Effect of nanoclay addition on the displacement-controlled flexural fatigue behavior of a polymer

A. Ramkumar · R. Gnanamoorthy

Received: 20 November 2009 / Accepted: 9 April 2010 / Published online: 23 April 2010

Abstract Reinforcing polymers with nanoclay improves the stiffness and decreases the dissipative nature of polymer matrix. This article describes the effect of nanoclay addition on the flexural fatigue response of Polyamide6 (PA6). The emphasis was on temperature rise, temperature-induced stiffness drop, and flexural fatigue life. The fatigue performance has been investigated under displacement-controlled flexural loading conditions at room temperature. The samples were subjected to same displacement amplitude and same initial force amplitude (force amplitude in the first fatigue cycle) flexural fatigue conditions. Under the same displacement amplitude conditions, PA6NC samples exhibited marginally lesser percentage drop in the initial force amplitude (temperature-induced stiffness change) compared to PA6. Due to the addition of nanoclay, a marginal improvement in fatigue life ($\sim$64,000 cycles) was also observed under these conditions. Under the same initial force amplitude conditions, PA6NC samples exhibited significantly lesser percentage drop in its initial force compared to PA6 and retained the stiffness throughout the fatigue life. In addition to this, a significant improvement in fatigue life (>150,000 cycles) was observed. The performance improvement due to nanoclay addition can be attributed to enhanced modulus coupled with reduced dissipation factor (tan δ) and improved surface hardness. The fibrillated appearance of the PA6NC fracture surface suggests that the clay addition promotes toughening and influences the crack propagation characteristics of PA6.

A. Ramkumar
Department of Mechanical Engineering, Indian Institute of Technology Madras, Chennai 600 036, India

R. Gnanamoorthy (✉)
Indian Institute of Information Technology, Design and Manufacturing (IIITD&M Kancheepuram), IIT Madras Campus, Chennai 600 036, India
e-mail: gmoorthy@iitm.ac.in

Introduction

One of the ways of improving the mechanical properties of polymers such as strength and stiffness is the incorporation of nanosized inorganic fillers into the virgin polymer matrix. Nanocomposite is a new class of high performance plastic material wherein at least one dimension of reinforcement is of the order of 1–100 nm and has been the material of recent interest. A complete review from preparation to processing of nanocomposites is presented by Ray and Okamoto [1]. An increase in modulus, tensile strength, and decrease in strain at yield due to the addition of nanoclay in polyamides is reported by Srinath and Gnanamoorthy [2]. Polymers dissipate part of mechanical energy in thermal form and depending upon the load and frequency, one can observe appreciable temperature rise when these materials are subjected to cyclic loading. Temperature rise results in loss of strength, stiffness, and eventually leads to failure of the component before the designed service life. Therefore, to design components efficiently or to replace an existing plastic with an advanced plastic like nanocomposites, thorough understanding of material behavior under cyclic loading conditions is imperative. The effect of nanoclay addition on axial fatigue behavior of polyamide 6 (PA6) was reported in the previous study [3]. Isocyclic stress strain diagrams were used to compare the fatigue behavior. Polyamide 6 nanocomposite (PA6NC) samples were found to exhibit a reduced modulus drop and lesser temperature rise compared to PA6 during fatigue. Alexandre and Dubois [4] performed a comprehensive study on polymer-layered

silicate nanocomposites that includes preparation, properties, and uses of these new classes of materials. Fornes and Paul [5] explained the origin of the superior reinforcing efficiency observed in well-exfoliated polymer–clay nanocomposites compared to conventional composites using composite theory. Authors used the theories of Halpin–Tsai and Mori–Tanaka and compared the predictions with experimental morphological and mechanical properties. Chavarria and Paul [6] investigated the effect of polyamide type and processing temperature on the mechanical properties and the morphology of nanocomposites formed from organically modified layered silicates by melt processing. Nanocomposites based on PA6 were found to exhibit better exfoliated structure and hence superior mechanical properties compared to those based on PA66 which exhibited a mixture of intercalated and exfoliated structures. A few authors conducted studies on the long-term mechanical behavior of polymer nanocomposites. Zhang et al. [7] showed that the addition of even a very low volume content of 21 nm-TiO_2 particles in a polyamide 6,6 (PA6,6) matrix could remarkably improve the creep behavior of unreinforced PA6,6 under various creep loads at both room and elevated temperature. The nanocomposites were found to exhibit lesser creep strain and longer creep life compared to unreinforced polymer. Rao and Pochan [8] studied the mechanics of polymer nanocomposites system and reported the existence of a strong interfacial interaction between the polymer chain and the nanoclay filler due to the incorporation of nanoclay. Bureau et al. [9] characterized the dispersion of the clay particles at the microscopic scale in the polypropylene/clay nanocomposites and studied the mechanical behavior of the polypropylene/clay nanocomposites with emphasis on the fracture toughness and fractographic analysis. Manjunatha et al. [10] investigated the tensile fatigue behaviour of micron-rubber and nano-silica particle modified epoxy polymers and showed that the addition of either the 9 wt% carboxyl-terminated butadiene-acrylonitrile (CTBN) rubber micro-particles or the 10 wt% silica nano-particles alone in the epoxy polymer could enhance the fatigue life by a factor of about 3–4 times. The fracture surface analysis in that study revealed that the nano-silica filled epoxy polymers exhibited particle debonding-plastic void growth mechanism during the fatigue crack propagation stage. Cyclic loading of polymeric solids depending upon the combination of parameters like stress amplitude, frequency, and temperature may result in continuous rise of temperature leading to thermal failure as opposed to conventional fatigue cracking. A few authors have reported such thermal failure mechanism during fatigue loading of polymers [11–13]. Bellemare et al. [11] reported the effect of nanoparticle addition on the fatigue crack initiation and propagation mechanisms and on the axial fatigue properties of polyamide. The nanocomposite samples were found to endure greater number of fatigue cycles than non-filled polyamide 6. Authors have also reported thermal instability phenomenon during fatigue of polyamide 6 nanocomposites at high stress regimes. Crawford and Benham [12] investigated the fatigue behavior of acetal copolymer along with the thermal aspects of failure. An attempt was made using theoretical and empirical methods to predict the possibility of thermal softening failure under given loading conditions. Mallick and Zhou [13] investigated the fatigue and tensile characteristics of polypropylene and polyamide nanocomposite and reported the strain rate and temperature dependency of yield strength and modulus. Polyamide nanocomposites were found to exhibit higher fatigue strength than polypropylene nanocomposites.

The polymer-layered silicate nanocomposite system has been well characterized in terms of strength, stiffness, and even impact/crash resistance. However, only a few authors have investigated the effect of nanoclay addition on the fatigue performance of polymer matrix. This article describes the effect of nanoclay reinforcement on the flexural fatigue performance of polyamide 6 under displacement-controlled conditions at room temperature. The effect of nanoclay addition was studied in terms of temperature rise, temperature-induced stiffness drop, and fatigue life. The fracture morphology is discussed.

Material and experimental methods

Test materials

In the current study, commercial grade polyamide 6 pellets and hectorite clay, which is organically modified with hydrogenated tallow quaternary amine complex, were used. The layer thickness of hectorite clay particle is around 1 nm and the particle length ranges from 200 to 300 nm [1]. PA6 pellets and clay (5% wt) were mixed thoroughly in a screw mixer and fed into a Bernstoff co-rotating twin-screw extruder. The temperatures at the six heating zones were maintained at 448, 468, 473, 493, 513, and 523 K, respectively. Rotational speed of the screws was maintained at 125 rpm. The hot extrudate from the extruder was cooled by passing it through a water bath. The extrudate was cooled and then chopped into nanocomposite pellets. Pellets were dried in a chamber at 333 K to remove any traces of moisture before molding. Injection molding was carried out at an injection pressure of 125 MPa and a melt temperature of 513 K. Flexural fatigue specimens according to ASTM D 671-71 dimensions were injection molded. The geometry of the specimen is such that, for a given end displacement, the specimen experiences uniform bending stress on its outer fibers. The span length for flexure is 30 mm and the thickness

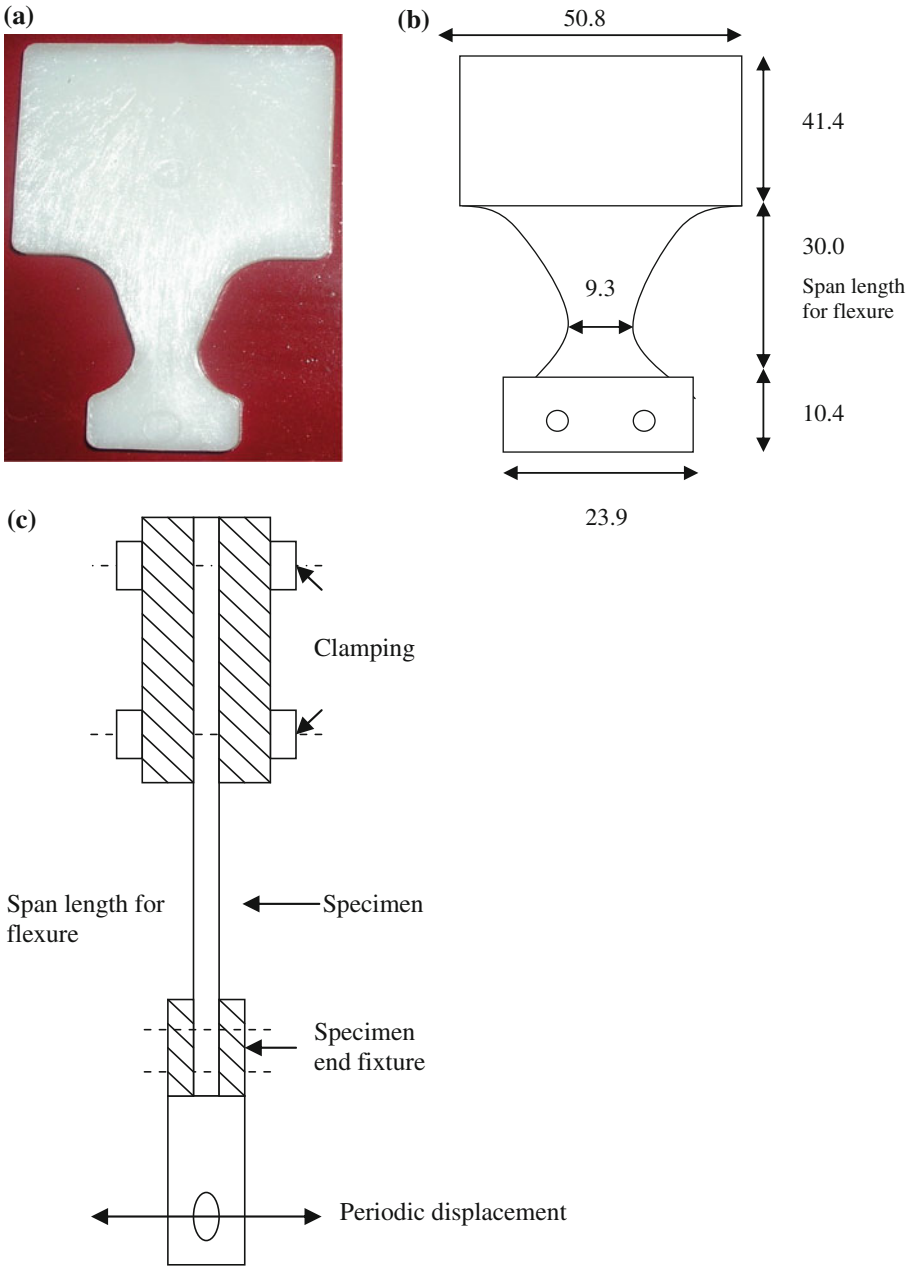

Fig. 1 **a** Photograph of the injection molded flexural fatigue specimen. **b** Schematic picture showing the dimensions of the fatigue specimens. **c** Schematic of specimen clamping procedure

of the sample is 3.6 mm. Figure 1a, b shows the image and the dimensions of the specimens used for the fatigue study. Fatigue specimens were conditioned at 323 K for 4 h before the commencement of tests. Tensile tests conducted at a constant crosshead rate of 1.5 mm/min revealed an increase in the elastic modulus of about three times in nanocomposites compared to unfilled polyamides. Tensile strength increased by about 50% with the addition of nanoclay [3]. The molded samples were characterized using Shimadzu X-ray diffractometer. A diffraction peak at 3.9° was observed in the XRD pattern of organoclay, which corresponds to the characteristic gallery spacing between the clay platelets. This peak is not discernable in the pattern of PA6NC, which indicates that the silicate sheets in the nanocomposite are completely dispersed in the matrix resulting in a completely exfoliated structure. The details of the XRD analysis were also reported in the previous study [3].

Experimental

Although most of the fatigue experiments were performed under load-controlled mode, displacement-controlled experiments have a distinctive advantage especially in polymer fatigue. Loss of material stiffness (due to

hysteretic heating) during displacement-controlled fatigue manifests itself as decrease in force amplitude and therefore temperature rise during such experiments stabilizes invariably [12]. This ensures that the samples fail mostly due to mechanical fatigue rather than the thermal failure. In the present study, displacement-controlled cantilever bending fatigue tests were carried out in alternate bending ($R = -1$) mode. The displacement amplitude for the tests (20 and 16 mm) was selected such that nominal stresses at the minimum cross section are less than the corresponding yield strength of the materials. The cyclic waveform used was triangular and the test frequency was maintained at 2 Hz. Temperature was recorded in the most constrained part of the sample using a calibrated non-contact infrared temperature sensor. Minimum of three samples were tested for each material and average values of the results were reported. Load and displacement as a function of time were recorded using a data acquisition system and a personal computer. Figure 1c shows the schematic of the clamped specimen. The fatigue performance was investigated at two different loading conditions under *displacement* control mode; (i) same displacement amplitude conditions, where both PA6 and PA6NC were fatigued at displacement amplitude of 20 mm. Under these conditions, the initial force amplitude experienced by the samples differs, due to difference in their stiffnesses and (ii) same initial force amplitude conditions, where PA6NC is fatigued at a reduced displacement of 16 mm. The objective of this is to subject PA6NC samples to the same initial force amplitude as that experienced by PA6 at displacement amplitude of 20 mm.

Results and discussion

Fatigue behavior under same displacement amplitude

Cyclic loading of polymeric materials results in internal heat generation due to their viscoelastic nature. The area enclosed in a force–displacement loop obtained during the fatigue tests of polymers represents the heat generated in a cycle. As the specimens in the present study, were loaded under constant displacement amplitude conditions, drop in material rigidity (due to thermal softening) resulted in a drop in the force amplitude. This can be visualized in Figs. 2, 3, i.e., hysteresis loops obtained during the fatigue tests for PA6 and PA6NC samples, respectively. The slope of the hysteresis loop decreased continuously during the initial cycles due to hysteretic heating and stabilized when the thermal equilibrium (constant temperature) was reached. Accordingly, temperature measurements revealed a rapid rise during the initial cycles for both the samples and remained stabilized for a good part of the specimen life. However, temperature of PA6 samples stabilized at

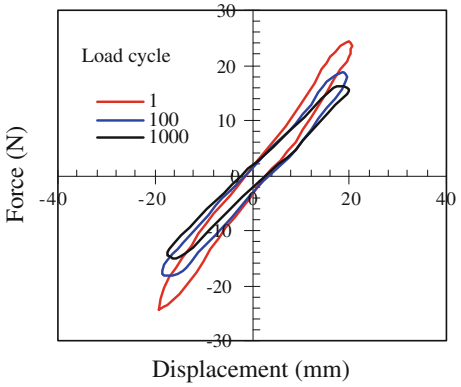

Fig. 2 Hysteresis loops corresponding to first, 100th, and 1,000th cycle during fatigue of PA6 at displacement amplitude of 20 mm

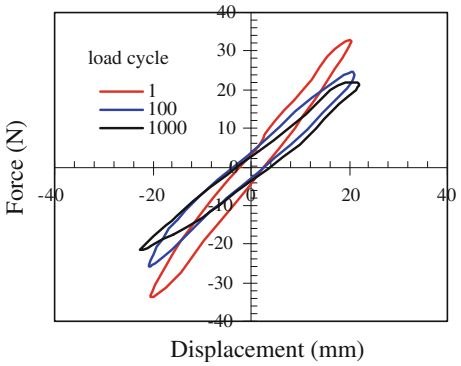

Fig. 3 Hysteresis loops corresponding to first, 100th, and 1,000th cycle during fatigue of PA6NC at displacement amplitude of 20 mm

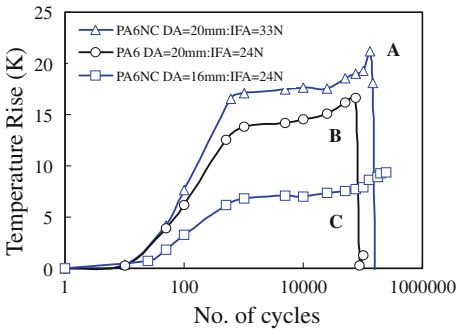

Fig. 4 Temperature rise with respect to number of cycles

~318 K, whereas PA6NC experienced a stable temperature of ~327 K (curves A and B in Fig. 4). Steady state loops were observed from 1,000th cycle. Figure 5 shows the hysteresis loops for the first cycle observed in PA6 and PA6NC samples. As PA6NC samples experienced greater initial force amplitude, comparatively greater heat generation (i.e., greater loop area) and higher temperature rise was observed in these samples. To quantify the stiffness changes that occur during fatigue, force amplitude values

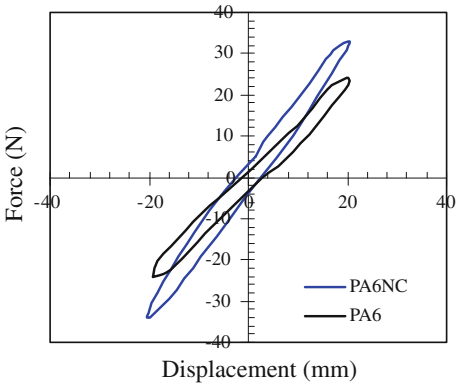

Fig. 5 Hysteresis loops for the first cycle observed in PA6 and PA6NC samples tested under the conditions of same displacement amplitude

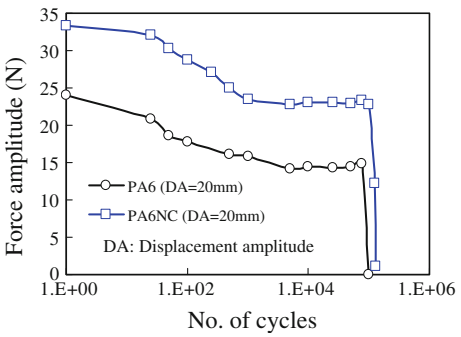

Fig. 6 Force amplitude variations with respect to number of cycles in PA6 and PA6NC samples during fatigue

were logged continuously during the tests. The variation of force amplitude with respect to number of cycles is shown in Fig. 6. Three distinct stages of force amplitude variation can be seen in both the samples investigated. In the first stage, there was a rapid drop in initial force amplitude due to the establishment of thermal regime (hysteresis heating). In spite of experiencing higher force amplitude and higher temperature rise during the first stage, PA6NC samples exhibited reduction of ~30% of its initial force amplitude (~34 N) whereas PA6 samples lost ~37% of its initial force amplitude (~24 N). Almost no variation in the force amplitude was observed during the second stage. A rapid drop in the force amplitude was observed during the third stage due to formation and propagation of fatigue cracks.

Fatigue behavior under same initial force amplitude

As PA6NC samples are stiffer than PA6, comparatively lesser displacement amplitude (16 mm) was required to impose initial force amplitude of 24 N in PA6NC. However, PA6 samples were fatigued at displacement amplitude of 20 mm to attain the same initial force amplitude.

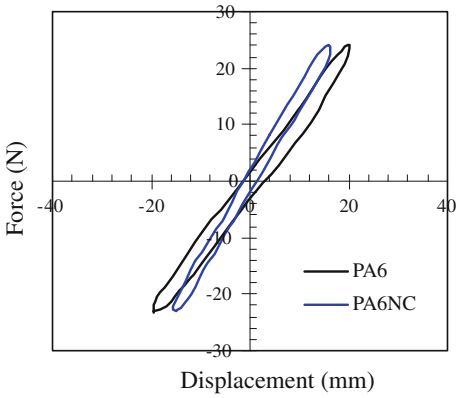

Fig. 7 Hysteresis loops for the first cycle in PA6 and PA6NC samples tested at initial force amplitude of 24 N

Figure 7 shows the hysteresis loops for the first cycle of the fatigue tests performed under the conditions of same initial force amplitude. SIGMAPLOT® was used to calculate the areas of the hysteresis loops and the values were found to be 184 Nmm for PA6 and 124 Nmm for PA6NC. Since this area represents the heat generated in the sample, the values suggest that the addition of nanoclay reduces heat generation by almost 30% under tested conditions. This reduction can be explained on basis of loss tangent values of the materials. The loss tangent, which is a measure of dissipative nature of material, is found to be comparatively lower for nanocomposites samples, i.e., $\tan\delta = 0.114$ (PA6NC), $\tan\delta = 0.14$ (PA6). Many authors [4, 8] in the past have observed improvement in dynamic mechanical properties and attributed it to the existence of strong interaction between the clay particle and the surrounding matrix resulting in effective transfer of stress at nanolevel. Therefore, in the current study, reduction of loss tangent and reduced displacement amplitude for a given force amplitude condition, which is brought about by increased stiffness, contributes to the overall reduction in hysteresis heating in PA6NC. As can be seen in Fig. 4 (comparing curves B and C), both the samples experienced a rapid rise in temperature during initial stages followed by a stable period. However, due to the reduction of hysteresis heat generation, PA6NC experienced a lesser temperature rise than PA6 and the shape, size, and environmental conditions being same for both the samples. Figure 8 shows the variation of force amplitude with respect to number of cycles for PA6NC samples tested at an initial force amplitude of 24 N (displacement amplitude = 16 mm). Force amplitude variation of PA6 samples tested at displacement amplitude of 20 mm was also included in the plot for comparison. During the early stages of fatigue (thermal regime), a drop of only ~3 N was observed in the PA6NC samples whereas a drop of ~9 N was observed in PA6 samples. The results emphasize the fact that overall benefits of

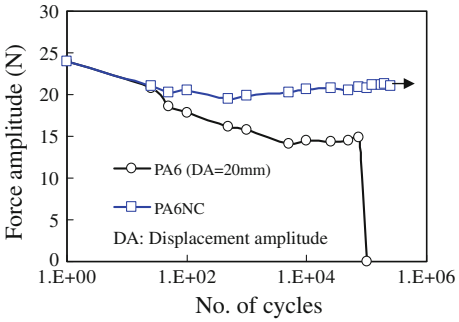

Fig. 8 Force amplitude variations with respect to number of cycles observed in PA6 and PA6NC samples tested at initial force amplitude of 24 N

nanoclay addition has its origin in stiffness improvement, i.e., stiffening effect due to incorporation of nanoclay results in lower heating during the initial cycles, and this leads to reduced drop in force amplitude in the subsequent cycles. This is a desirable aspect because, if polymers are subjected to load-controlled fatigue, the temperature rise during the initial stages results in stiffness drop which in turn increases the heat dissipation in the subsequent cycles [12]. Therefore, if one can limit the temperature rise during the initial stages by using a stiffer material, stiffness drop during subsequent stages of fatigue can be minimized. A stiffer, stronger material also helps in weight reduction.

Flexural fatigue life

The nominal stresses near the minimum cross section of the samples were calculated using a simple beam model and normalized with the respective yield strength of the materials [13]. Measured force data, i.e., force amplitude corresponding to 99% of the fatigue life (Fig. 6) was used for this and the values were found to be $\sigma_b = 23.9$ MPa for PA6NC and $\sigma_b = 14.93$ MPa for PA6. Table 1 shows the summary of fatigue life details of the specimens. Under the *same displacement amplitude conditions*, the average life of the PA6 samples tested was found to be ~90,000 cycles while that of PA6NC samples was ~154,000 cycles. There is a marginal improvement in fatigue life although the PA6NC specimens experienced higher force amplitude compared to PA6 (with normalized stress being same). Under the *same initial force amplitude conditions*, the fatigue life of PA6NC exceeded 250,000 cycles at initial force amplitude of 24 N while the average life of PA6 was only 90,000 cycles. Fatigue studies conducted on PA6NC by Bellemare et al. [11] suggested that the overall improvement in fatigue life due to nanoclay addition could be attributed to the enhancement of material resistance to crack initiation. Moreover, in the previous study [3] the nanoparticles were found to increase the tensile strength ($\sigma_{t,PA6} = 34$ MPa, $\sigma_{t,PA6NC} = 52$ MPa) and modulus of PA6. This increase in tensile strength and modulus reduces the cyclic straining of the polymer molecules during fatigue and probably contributes to improved fatigue performance, with processing and testing conditions being same for both the samples [3, 11]. In addition, PA6NC was found to exhibit comparatively a harder molding skin than PA6, i.e., shore-D hardness of PA6NC = 84 and shore-D hardness of PA6 = 73. This may be another factor contributing to the enhanced resistance to crack initiation.

Table 1 Details of the stresses induced (analytical calculations) and fatigue life of the test samples under the conditions of same displacement amplitude

Material	PA6	PA6NC
Nominal stress near the minimum cross section	15 MPa	24 MPa
Normalized stress (σ/σ_y)	0.44	0.46
Fatigue life of individual specimen (cycles)	97,500	163,100
	82,000	144,800
	90,200	153,100
Average (cycles)	89,900	153,666

Fracture mechanisms

Fatigue cracks were observed to initiate at the edges near the minimum cross section and propagate diagonally across the specimens in both the materials (Fig. 9). Figures 10 and 11 show the photograph of the failed specimens. As can be seen, fracture plane in both the samples is nearly perpendicular to the direction of the bending stress. Fracture surface of PA6NC shows two distinct regions, i.e., a macroscopically flat smooth crack initiation region and a rough final fracture region (Fig. 12) whereas fracture surface of PA6 shows comparatively smooth morphology throughout (Fig. 13). Such fracture surfaces have been previously observed in polymer nanocomposites. For example, Bellemare et al. [11] observed smooth central crack initiation region surrounded by rough and inclined final fracture region in fractured axial fatigue samples of PA6NC. Figure 14 shows the SEM picture of PA6NC

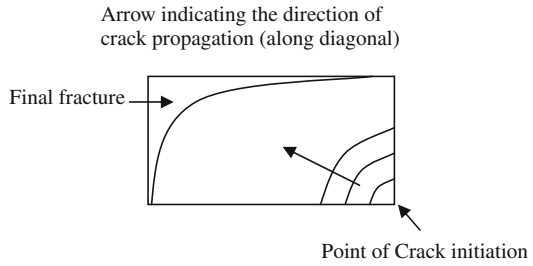

Fig. 9 Schematic of the crack propagation mechanism

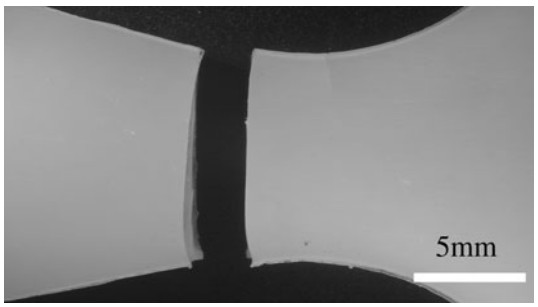

Fig. 10 Photograph of fractured PA6 specimen

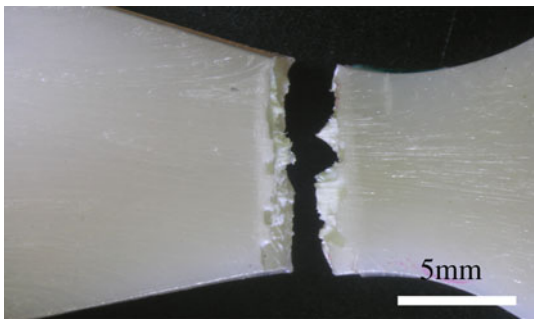

Fig. 11 Photograph of fractured PA6NC specimen

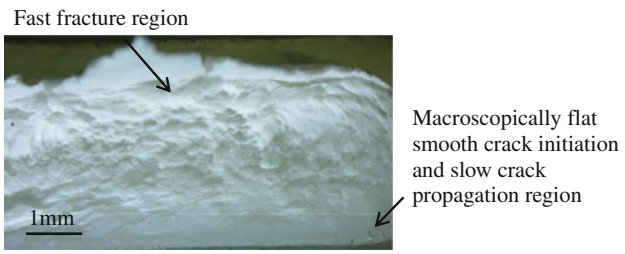

Fig. 12 Fracture surface of PA6NC showing two distinct regions

Fig. 13 Fracture surface of PA6 showing smoother morphology

taken at a point 2 mm diagonally away from crack initiation. The image displays a fibrillated appearance, i.e., rough texture with arrays of dimples or voids approximately 40–80 μm in size and significant tearing of fibrils at their periphery. Similar fibrillation mechanism in polypropylene nanocomposites has been previously reported by

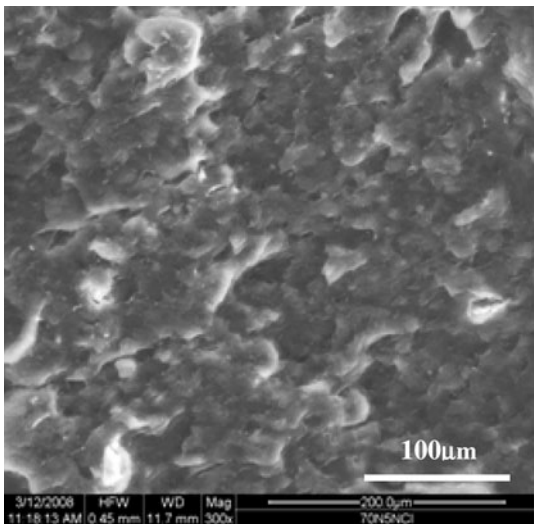

Fig. 14 Fibrillated deformation zone observed at a point 2 mm diagonally away from crack initiation point in PA6NC

Bureau et al. [9]. In that particular study, clay reinforced polypropylene was found to exhibit greater fibrillation than unreinforced polypropylene and it was showed that the increased fibrillation could be a manifestation of increased plastic work. In another work, Manjunatha et al. [10] observed fatigue fracture surface of silica nanoparticle filled epoxy exhibiting a rough fracture surface with plastic void growth and neat epoxy exhibiting a relatively smooth fracture and is devoid of large-scale plastic deformation. The improvement in fatigue life of nano-silica filled epoxy was attributed to this particle toughening. As can be seen in Fig. 15, SEM image of PA6 at the same point reveals a smoother morphology and no fibrillated deformation zone

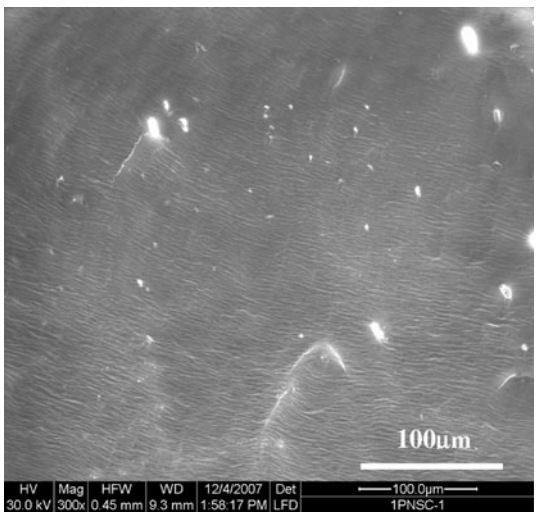

Fig. 15 SEM image of PA6 fracture surface at a point 2 mm diagonally away from crack initiation point showing smoother morphology

similar to those observed in PA6NC. This clearly shows that the addition of nanoclay can promote toughening and may prove to be effective in slowing damage propagation, as a significant fraction of strain energy must be expended in fibrillation process.

Conclusions

Displacement-controlled flexural fatigue studies were conducted on PA6 and PA6NC samples under two different loading conditions. Under the conditions of same displacement amplitude, PA6NC samples endured marginally greater fatigue cycles compared to PA6. During the initial stages of fatigue, PA6 samples exhibited marginally greater percentage reduction in its initial force amplitude in spite of experiencing lesser temperature rise compared to PA6NC. Under the same initial force amplitude conditions, PA6NC samples showed lesser temperature rise and lower reduction in force amplitude compared to PA6. The nanoclay reinforcement was found to be effective for substantial reduction of hysteresis heat and significant improvement in fatigue life.

References

1. Ray SS, Okamoto M (2003) Prog Polym Sci 28:1539
2. Srinath G, Gnanamoorthy R (2005) J Mater Sci 40:2897. doi:10.1007/s10853-005-2439-0
3. Ramkumar A, Gnanamoorthy R (2008) Compos Sci Technol 68:105
4. Alexandre M, Dubois P (2000) Mater Sci Eng 28:1
5. Fornes TD, Paul DR (2003) Polymer 44:4993
6. Chavarria F, Paul DR (2004) Polymer 45:8501
7. Zhang Z, Yang JL, Friedrich K (2004) Polymer 45:3481
8. Rao Y, Pochan JM (2007) Macromolecules 40:290
9. Bureau MN, Perrin-Sarazin F, Ton-That MT (2004) Polym Eng Sci 44(6):1142
10. Manjunatha CM, Taylor AC, Kinloch AJ, Sprenger S (2009) J Mater Sci 44:4487. doi:10.1007/s10853-009-3653-y
11. Bellemare SC, Bureau MN, Denault J, Dickson JI (2004) Polym Compos 25(4):433
12. Crawford RJ, Benham PP (1974) J Mater Sci 9:18. doi:10.1007/BF00554752
13. Mallick PK, Zhou Y (2003) J Mater Sci 38:3138. doi:10.1023/A:1025161215708